

# Effects of tungsten thickness and annealing temperature on the electrical properties of W–TiO<sub>2</sub> thin films

Chia-Ching Wu<sup>a</sup>, Cheng-Fu Yang<sup>b,\*</sup>, Yuan-Tai Hsieh<sup>c</sup>, Wen-Ray Chen<sup>d</sup>,  
Chin-Guo Kuo<sup>e</sup>, Hong-Hsin Huang<sup>f</sup>

<sup>a</sup> Department of Electronic Engineering, Kao Yuan University, Kaohsiung, Taiwan, ROC

<sup>b</sup> Department of Chemical and Materials Engineering, National University of Kaohsiung, Kaohsiung, Taiwan, ROC

<sup>c</sup> Department of Electronic Engineering, Southern Taiwan University, Tainan, Taiwan, ROC

<sup>d</sup> Department of Electronic Engineering, National Formosa University, Yunlin, Taiwan, ROC

<sup>e</sup> Department of Industrial Education, National Taiwan Normal University, Taipei, Taiwan, ROC

<sup>f</sup> Department of Electrical Engineering, Cheng Shiu University, Kaohsiung, Taiwan, ROC

Received 4 March 2011; received in revised form 26 April 2011; accepted 4 May 2011

Available online 5th July 2011

## Abstract

TiO<sub>2</sub> thin films were prepared by RF magnetron sputtering onto glass substrates and tungsten was deposited onto these thin films (deposition time 15–60 s) to form W–TiO<sub>2</sub> bi-layer thin films. The crystal structure, morphology, and transmittance of these TiO<sub>2</sub> and W–TiO<sub>2</sub> bi-layer thin films were investigated. Amorphous, rutile, and anatase TiO<sub>2</sub> phases were observed in the TiO<sub>2</sub> and W–TiO<sub>2</sub> bi-layer thin films. Tungsten thickness and annealing temperature had large effects on the transmittance of the W–TiO<sub>2</sub> thin films. The W–TiO<sub>2</sub> bi-layer thin films with a tungsten deposition time of 60 s were annealed at 200 °C–400 °C. The band gap energies of the TiO<sub>2</sub> and the non-annealed and annealed W–TiO<sub>2</sub> bi-layer thin films were evaluated using  $(\alpha h\nu)^{1/2}$  versus energy plots, showing that tungsten thickness and annealing temperature had major effects on the transmittance and band gap energy of W–TiO<sub>2</sub> bi-layer thin films.

Crown Copyright © 2011 Published by Elsevier Ltd and Techna Group S.r.l. All rights reserved.

**Keywords:** A. Films; C. Electrical properties; C. Ferroelectric properties; D. TiO<sub>2</sub>

## 1. Introduction

Titanium dioxide (TiO<sub>2</sub>) is widely studied because of its ability to photo-oxidize harmful chemicals to CO<sub>2</sub> in both air and water in the presence of UV light. TiO<sub>2</sub> also shows promise for energy applications such as water splitting [1] and photochemical solar cells [2]. Despite the many potential applications of TiO<sub>2</sub>, wider practical use requires that its photo-response be farther extended into the visible light region and its photo-efficiency be increased by reducing charge recombination. It is therefore interesting to explore the structure, phase, and orientation of TiO<sub>2</sub> thin films. Visible light response is a very important factor when examining TiO<sub>2</sub> as a photocatalyst, and the band gap energy value is a key property for photocatalytic activity.

In the past, many methods were developed to shift the band gap energy of rutile phase TiO<sub>2</sub> to a visible light range. Thin film coating of photocatalytic TiO<sub>2</sub> via various processes is a key technology for the practical use of this material. One method is adding other materials as dopants; another method is fabricating TiO<sub>2</sub>-based multi-layer thin films. For example, many studies have incorporated different dopants, such as Fe [3,4], Mo, Ru, Os, Re, V, Rh, Co, and Al [4], SiO<sub>2</sub> [5], as well as Cr and Mo [6], into TiO<sub>2</sub> substrates by various mixing and coating techniques to increase the photocatalytic sensitivity in UV and visible light environments. Many metals, such as Ag [7], Ni, Cu, V, and Fe [8], can also be deposited onto TiO<sub>2</sub> thin films to form a bi-layer structure, thereby shifting the band gap energy of the rutile phase of TiO<sub>2</sub>. In this study, tungsten (W) was deposited on TiO<sub>2</sub> thin films to form W–TiO<sub>2</sub> bi-layer thin films. The effects of tungsten deposition time (thickness) on transmittance and on the crystal structure of TiO<sub>2</sub> thin films in the bi-layer structure were studied. For comparison, W–TiO<sub>2</sub> thin films (tungsten deposition time:

\* Corresponding author..

E-mail address: [cfyang@nuk.edu.tw](mailto:cfyang@nuk.edu.tw) (C.-F. Yang).

60 s) were also annealed in air at different temperatures. The effect of annealing temperature on the characteristics of W–TiO<sub>2</sub> thin films was also investigated.

## 2. Experimental procedure

Polyvinylalcohol (PVA) was added into the TiO<sub>2</sub> powder as a binder and the mixture was uniaxially pressed into pellets in a steel die. After debinding, sintering of the TiO<sub>2</sub> ceramic was carried out at 1400 °C for 4 h. An X-ray diffraction pattern of TiO<sub>2</sub> ceramic in the rutile phase was obtained. TiO<sub>2</sub> single-layer and W–TiO<sub>2</sub> bi-layer thin films were deposited onto well-cleaned glass substrates by RF magnetron sputtering at a pure argon work pressure of between  $5 \times 10^{-3}$  and  $5 \times 10^{-2}$  Torr. The working distance was 50 mm for the TiO<sub>2</sub> target and 120 mm for the tungsten target. First, the W–TiO<sub>2</sub> thin films were deposited at a glass substrate temperature of 150 °C. The deposition time for TiO<sub>2</sub> was 30 min and the time for the tungsten thin film was changed from 15 s to 60 s. The morphologies and thicknesses of the TiO<sub>2</sub> and W–TiO<sub>2</sub> bi-layer thin films were observed and measured by field effect scanning electron microscopy (FESEM) and the transmittance was measured by UV–vis–NIR spectrophotometry (HP-8453E). For comparison, the W–TiO<sub>2</sub> bi-layer thin films with a tungsten deposition time of 60 s were also annealed at 200–400 °C for 4 h.

## 3. Results and discussion

The surface morphology and microstructure of TiO<sub>2</sub> thin films depend closely on the final tungsten thickness (Fig. 1). The nano-crystalline TiO<sub>2</sub> grains grew significantly with increasing tungsten deposition time. The thicknesses of TiO<sub>2</sub>

and tungsten were measured from the cross-section images of TiO<sub>2</sub> and W–TiO<sub>2</sub> thin films shown in Fig. 2. The thickness of TiO<sub>2</sub> in the lower layer showed no apparent change, while the thicknesses of the W–TiO<sub>2</sub> thin films increased with increasing tungsten deposition time. For deposition times of 15, 30, and 60 s, the tungsten thickness was 14 nm, 26 nm, and 44 nm, respectively.

The XRD patterns of the W–TiO<sub>2</sub> thin films were investigated for different tungsten deposition times. As shown in Fig. 3, in the single-layer TiO<sub>2</sub> thin films, the rutile, anatase, and amorphous phases coexisted. After the tungsten was deposited to form the W–TiO<sub>2</sub> bi-layer thin films, those same TiO<sub>2</sub> phases also coexisted in the XRD patterns. Fig. 4(a) shows the UV–vis spectrum of the TiO<sub>2</sub> and W–TiO<sub>2</sub> bi-layer thin films in the wavelength range of 300–1100 nm. The prepared thin films had a high transparency ratio in the visible range of 400–700 nm, and the transparency apparently decreased with increasing tungsten thickness. As tungsten was deposited on the TiO<sub>2</sub> thin films to form W–TiO<sub>2</sub>, the absorption edge of the TiO<sub>2</sub> thin films was red-shifted. This result is ascribed to the tungsten, which caused a difference in the ratio of crystal phase transformation (Fig. 3), leading to a difference in the band gap energy of the TiO<sub>2</sub> thin films [9]. In the past, determination of the band gap energy ( $E_g$ ) was often necessary to develop the electronic band structure of a thin film material. In the high absorption region ( $>10^4 \text{ cm}^{-1}$ ), the absorption coefficient  $\alpha$  is related to the energy  $h\nu$  of incident photons as follows [10]:

$$\alpha = \left[ \frac{B(h\nu - E_g)^n}{h\nu} \right] \quad (1)$$

$$\alpha = \left[ \frac{1}{d} \ln \left( \frac{1}{T} \right) \right] \quad (2)$$

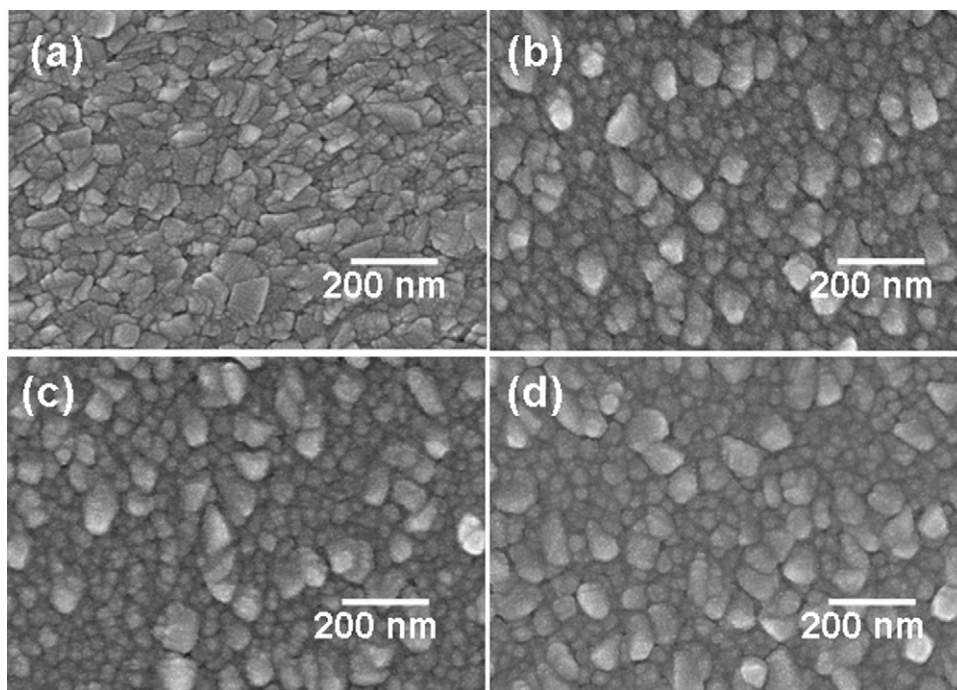


Fig. 1. Morphology of W/TiO<sub>2</sub> thin films for different tungsten deposition time. (a) 0, (b) 15, (c) 30 and (d) 60 s.

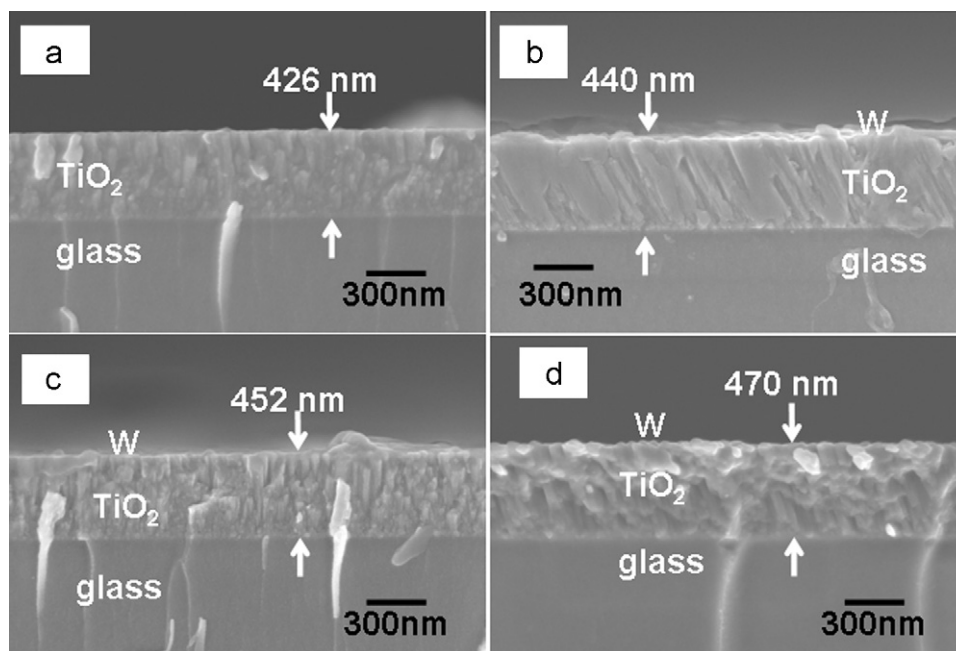


Fig. 2. Cross section observations of W-TiO<sub>2</sub> thin films for different tungsten deposition time. (a) 0 s, (b) 15 s, (c) 30 s, and (d) 60 s.

where  $B$  is a constant,  $p$  is an index that characterizes the optical absorption process,  $d$  is the thickness, and  $T$  is the transmittance ratio. At the shorter wavelengths close to the optical band gap, the fundamental absorption has a greater influence on  $\alpha$ .

In the high absorption region,  $\alpha$  is calculated with Eq. (2) using normal incident transmission data for the single-coated TiO<sub>2</sub> thin films. Fig. 4(b) illustrates the plots of  $(\alpha h\nu)^{1/2}$  against  $h\nu$  (energy) in accordance with Eq. (1);  $E_g$  can be found at  $(\alpha h\nu)^{1/2} = 0$ . Fig. 5 shows the calculated band gap energies of the TiO<sub>2</sub> and W-TiO<sub>2</sub> thin films. The band gap energy of the crystallite TiO<sub>2</sub> was about 3.21 eV, and the band gap energy of the W-TiO<sub>2</sub> bi-layer thin films decreased from 3.210 to 3.158 eV with increasing tungsten deposition time. From the

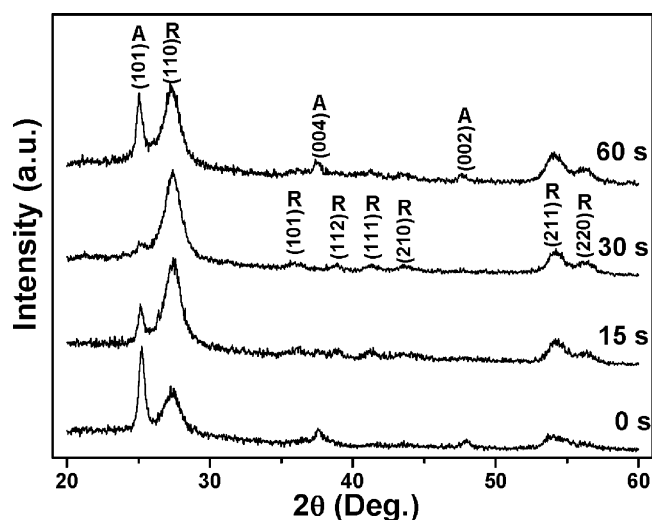


Fig. 3. X-ray diffraction patterns of W-TiO<sub>2</sub> thin films for different tungsten deposition time.

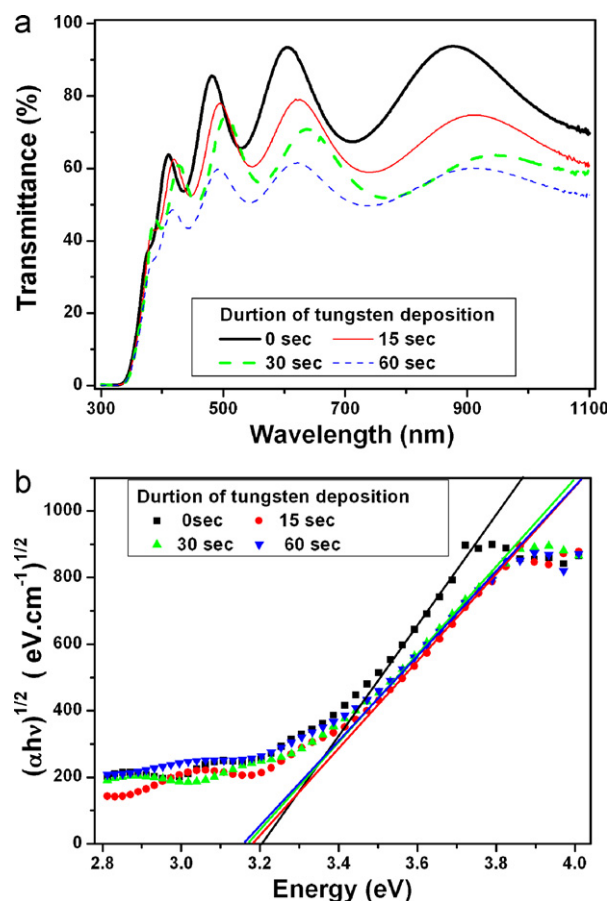


Fig. 4. (a) Transmittance and (b)  $(\alpha h\nu)^{1/2}$  plot of W-TiO<sub>2</sub> thin films for different tungsten deposition time.

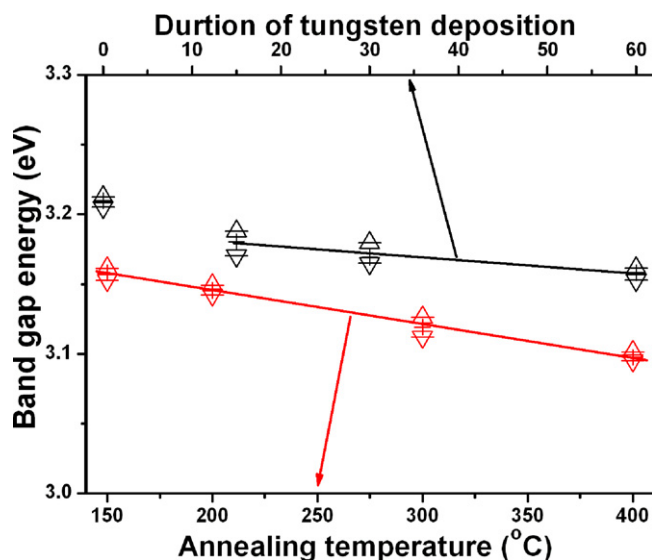


Fig. 5. Band gap energy of W-TiO<sub>2</sub> thin films for different tungsten deposition duration and annealing temperature.

XRD patterns shown in Fig. 3 it is evident that the rutile phase ratio for the W-TiO<sub>2</sub> bi-layer thin films changed as the tungsten deposition time increased. Because the band gap energy of the rutile phase is 3.0 eV, the existence of rutile

TiO<sub>2</sub> is not the only reason for the decrease in the  $E_g$  of the W-TiO<sub>2</sub> thin films; the addition of tungsten as the upper layer is another reason.

When the W-TiO<sub>2</sub> bi-layer thin films with a tungsten deposition time of 60 s were annealed at 200–400 °C, the surface morphologies underwent no apparent change. The UV–vis spectra of the W-TiO<sub>2</sub> bi-layer thin films are shown in Fig. 6 as a function of annealing temperature. As Fig. 6 shows, the transparency of the W-TiO<sub>2</sub> bi-layer thin films increased as the annealing temperatures rose. This result may be due to the tungsten diffusing into the TiO<sub>2</sub> layers, decreasing the thickness of the tungsten layer and increasing the transmittance ratio. Fig. 5 also shows that the calculated band gap energy of the annealed W-TiO<sub>2</sub> thin films decreased from 3.158 to 3.098 eV with rising annealing temperature. As this result suggests, annealing W-TiO<sub>2</sub> thin films is another method to decrease the band gap energy of TiO<sub>2</sub>-based thin films.

#### 4. Conclusions

The calculated results show that as the tungsten thickness and annealing temperature increased, the band gap energy values decreased. The band gap energy of deposited TiO<sub>2</sub> thin film was 3.21 eV. For the W-TiO<sub>2</sub> bi-layer thin films, as the tungsten deposition time was increased from 15 s to 60 s, the band gap energy shifted from 3.210 to 3.158 eV, which is in the range of visible light. When the annealing temperature of the W-TiO<sub>2</sub> bi-layer thin films was increased from 200 to 400 °C, the band gap energy shifted from 3.158 to 3.098 eV. Annealing was thus demonstrated to be another important method to decrease the band gap energy of TiO<sub>2</sub>-based thin films.

#### Acknowledgements

The authors will acknowledge to the financial support of NSC 99-2221-E-390-013-MY2 and the experimental data coordination of C.Y. Huang.

#### References

- [1] L. Chena, M.E. Grahamb, G. Lia, K.A. Graya, Fabricating highly active mixed phase TiO<sub>2</sub> photocatalysts by reactive DC magnetron sputter deposition, *Thin Solid Films* 515 (2006) 1176–1181.
- [2] M. Gratzel, Photoelectrochemical cell, *Nature* 414 (2001) 338–344.
- [3] J.A. Navio, G. Colon, M. Macias, C. Real, M.I. Litter, Iron-doped titania semiconductor powders prepared by a sol–gel method. Part I. Synthesis and characterization, *Applied Catalysis A: General* 177 (1999) 111–120.
- [4] W. Choi, A. Termin, M.R. Hoffmann, The role of metal ion dopants in quantum-sized TiO<sub>2</sub>: correlation between photoreactivity and charge carrier recombination dynamics, *The Journal of Physical Chemistry* 98 (1994) 13379–13669.
- [5] C.H. Kwon, J.H. Kim, I.S. Jung, H. Shina, K.H. Yoon, Preparation and characterization of TiO<sub>2</sub>–SiO<sub>2</sub> nano-composite thin films, *Ceramics International* 29 (2003) 851–856.
- [6] K. Wilke, H.D. Breuer, Influence of transition metal doping on the physical and photocatalytic properties of titania, *Journal of Photochemistry and Photobiology A: Chemistry* 121 (1999) 49–53.

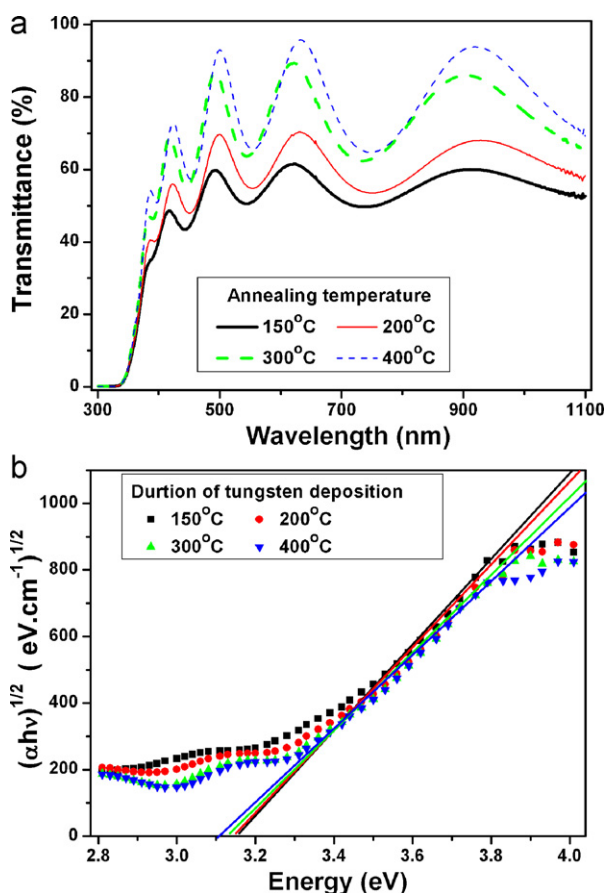


Fig. 6. (a) Transmittance and (b)  $(\alpha h\nu)^{1/2}$  plot of W-TiO<sub>2</sub> thin films for different annealing temperature.

- [7] Z. Wang, X. Cai, Q. Chen, P.K. Chu, Effects of Ti transition layer on stability of silver/titanium dioxide multilayered structure, *Thin Solid Films* 515 (2007) 3146–3150.
- [8] D.Y. Wang, H.C. Lin, C.C. Yen, Influence of metal plasma ion implantation on photo-sensitivity of anatase TiO<sub>2</sub> thin films, *Thin Solid Films* 515 (2006) 1047–1052.
- [9] T. Hashimoto, T. Yoko, S. Sakka, Sol–gel preparation and third-order nonlinear optical properties of TiO<sub>2</sub> thin films, *Bulletin of the Chemical Society of Japan* 67 (1994) 653–660.
- [10] M. Sreemany, S. Sen, A simple spectrophotometric method for determination of the optical constants and band gap energy of multiple layer TiO<sub>2</sub> thin films, *Materials Chemistry and Physics* 83 (2004) 169–177.